EREM 81/4
Journal of Environmental Research, Engineering and Management
Vol. 81 / No. 4 / 2025
pp. 120–130
10.5755/j01.erem.81.4.39917

Strategy for Maintaining Environmental Stability: Synthesis of CO_2 Emission Gases into Sodium Carbonate

Received 2024/12 | Accepted after revisions 2025/09

https://doi.org/10.5755/j01.erem.81.4.39917

Strategy for Maintaining Environmental Stability: Synthesis of CO_2 Emission Gases into Sodium Carbonate

Nuryoto Nuryoto[1]*, Heri Heriyanto[1], Rahmayetty Rahmayetty[1], Raihan Zikri Nawwari[1], Syahnaz Fatiyyah Harrisma[1], Rafiif Nur Tahta Bagaskara[2]

[1] Chemical Engineering Department, Faculty of Engineering, Universitas Sultan Ageng Tirtayasa, Indonesia

[2] School of Envinronment, Faculty of Arts and Science, University of Toronto, Canada

***Corresponding author:** nuryoto@untirta.ac.id

The growing urgency of global environmental issues and the critical role of green and sustainable chemistry in developing eco-friendly processes call for innovative strategies to minimize waste. The conversion of carbon dioxide (CO_2), the primary greenhouse gas, into high-value compounds such as sodium carbonate (Na_2CO_3) needs to be carried out by reacting it with sodium hydroxide (NaOH) in solution. Optimal CO_2 conversion can be achieved when integrating factors affecting the diffusion-reaction process is formulated correctly. Therefore, this research aims to analyze and investigate the extent influence of NaOH concentration, reaction temperature, and stirring speed in a pressurized system on the resulting Na_2CO_3. Observations were conducted across various variables to obtain comprehensive data and information. NaOH concentrations were tested in the range of 10–30wt%, stirring speeds of 200 and 300 rpm, and reaction temperatures of 20–50°C, with fixed variables of system pressure equivalent to 9.8 kPa and CO_2 gas flow rate of 2 liters/minute. To ensure Na_2CO_3 formation, characterization was performed using Fourier Transform Infrared Spectroscopy (FTIR) and Scanning Electron Microscopy (SEM). The results show that stirring speed, NaOH concentration, and system temperature can enhance the reaction rate and CO_2 diffusion in the solution, as evidenced by the increased production of Na_2CO_3. The highest conversion was achieved at a stirring speed of 300 rpm, NaOH concentration of 30wt%, and reaction temperature of 50°C, yielding 16.43 grams per 300 ml or equivalent to 54.77 grams per liter. FTIR and SEM test results were identical to the Na_2CO_3 product under optimal conditions. The method in this research offers an alternative process worth considering, as it can produce relatively high yields. However, further observations are still needed by combining NaOH concentration and CO_2 flow rate to make the process more effective, efficient, and economical.

Keywords: diffusivity, chemical reaction, steady state, reaction order, absorption.

Introduction

Climate change due to increasing CO_2 emissions in the atmosphere has become a global problem. High levels of CO_2 in the atmosphere trigger the greenhouse effect and will accelerate global warming (Couespel et al., 2024; Rogelj and Lamboll, 2024). CO_2 emissions originate from human activities, primarily industrial processes (Prajapati et al., 2024). Utilizing CO_2 as a raw material to produce valuable products is a promising and cost-effective approach that offers added value. The success of these actions will contribute to reducing carbon footprint, improving process economics sustainably, and creating new job opportunities. There are many types of greenhouse gases, namely CO_2, methane (CH_4), nitrogen oxides (NO_x), and fluorinated gases. CO_2 accounts for the majority of greenhouse gas emissions at 76%, while the remaining emissions consist of CH_4 at 16%, NO_x at 6%, and fluorinated gases at 2% (Ozerdem and Ozerdem, 2024). Therefore, maintaining the stability of CO_2 levels in the atmosphere becomes very important and necessary. Creating alternative technology using CO_2 as a raw material for a process is a concrete step to address this problem. This research attempts to transform CO_2 into Na_2CO_3 by contacting CO_2 gas with a liquid phase substance in NaOH solution. This process has strong potential for success due to the high solubility of NaOH in water and the ability to optimize CO_2 gas solubility by controlling key factors in the absorption process, allowing the reaction between NaOH and CO_2 to proceed efficiently and produce Na_2CO_3.

Theoretically, the synthesis of Na_2CO_3 from CO_2 and NaOH can be written as in *Equation (1)* (Chan et al., 2025).

$$CO_2 + 2NaOH \leftrightarrow Na_2CO_3 + H_2O \qquad (1)$$

The reaction in *Equation (1)* proceeds through an intermediate reaction mechanism, so it is not a direct reaction but instead proceeds through reactions as shown in *Equations (2)* and *(3)* (Evans et al., 2024).

$$CO_2 + Na^+ + OH^- \rightarrow NaHCO_3 \qquad (2)$$

$$NaHCO_3 + Na^+ + OH^- \rightarrow Na_2\,CO_3 + H_2O \qquad (3)$$

Therefore, proper operating conditions are needed for maximum Na_2CO_3 product formation, and the reaction products should not stop at the intermediate product $NaHCO_3$. The reaction product in the form of Na_2CO_3 can later be widely utilized, including as a food additive (Plaza et al., 2004), precursor adsorbent (Al-Mamoori et al., 2023), and catalyst (Rubangakene et al., 2023). Thus, the added value generated from converting CO_2 to Na_2CO_3 is quite substantial. In addition, this process has the potential to be applied on an industrial scale due to its simplicity, the use of readily available raw materials, and the absence of extreme operating conditions. From an economic standpoint, CO_2 capture using this method can reduce production costs by utilizing a semi-continuous system without complex stages. From an environmental perspective, the CO_2 capture process supports efforts to reduce carbon emissions through the direct conversion of CO_2 into valuable products. Therefore, this research can serve as an initial bridge toward the broader industrial application of NaOH-based CO_2 conversion.

The reaction between CO_2 and NaOH solution is classified as a heterogeneous reaction and is governed by the diffusion-reaction mechanism (refer to *Fig. (1)*). The rate of this reaction depends on how quickly CO_2 bubbles can diffuse into the NaOH solution. Efficient interaction between CO_2 and NaOH occurs when the diffusion process is fast and unobstructed.

Fig. 1. *Illustration of the diffusion-reaction phenomenon between CO_2 and NaOH*

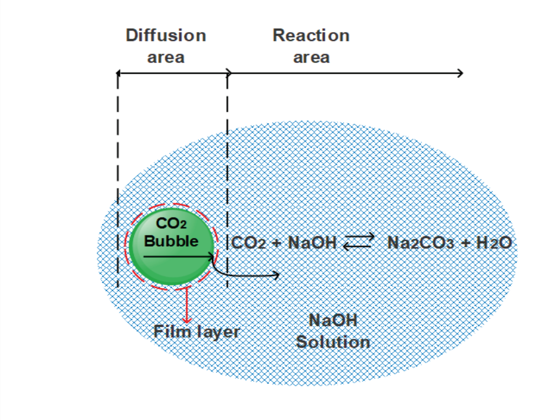

The diffusion-reaction concept in *Fig. (1)* can be explained using empirical equations presented in *Equations (4) – (5)* (referring to Fogler, 2006).

$$-\frac{dC_{CO_2}}{dt} = D\,\frac{dC_{CO_2}}{\delta} \qquad (4)$$

$$-\frac{dC_{CO_2}}{dt} = k_1\,C_{CO_2}\,C_{NaOH} - k_2\,C_{Na_2CO_3}\,C_{H_2O} \qquad (5)$$

When the reaction system conditions have reached steady state, diffusion rate will be equal to the reaction rate, and *Equation (4) – (5)* can be simplified to *Equation (6)*.

$$D\,\frac{dC_{CO_2}}{\delta} = k_1\,C_{CO_2}\,C_{NaOH} - k_2\,C_{Na_2CO_3}\,C_{H_2O} \tag{6}$$

where C_{CO^2} – concentration of CO_2 (mol/L); – concentration of NaOH (mol/L); $C_{Na^2CO^3}$ – concentration of Na_2CO_3 (mol/L); C_{H^2O} – concentration of H_2O (mol/L); δ – film layer (dm); D – diffusivity coefficient (dm^2/s); $\frac{dC_{CO_2}}{dt}$ – diffusion rate and reaction rate (mol/L·s); k_1 – reaction rate constant in the forward direction (L/(mol·s); k_2 – reverse reaction rate constant (L/(mol·s).

Research on CO_2 capture using NaOH solution to reduce CO_2 gas emissions and produce Na_2CO_3 has experienced relatively rapid development (see *Table 1*). However, most previous studies were carried out under atmospheric pressure without stirring, which led to suboptimal CO_2 capture results (See Table 1). Under these conditions, the diffusion-reaction process is limited, resulting in lower product yields. Additionally, many of the studies focused solely on material characterization without providing quantitative data on the final product (Guchhait et al., 2022). In some cases, the reaction only produced intermediate compounds such as $NaHCO_3$ (Kuliyev et al., 2023), indicating that the conversion process was not yet fully optimized. Therefore, this research attempts to observe and integrate these factors (pressure and stirring speed) with NaOH concentration and reaction system temperature factors. This action was taken based on the theoretical concepts written in *Equations (5) – (8)* (Bird et al., 2002; Fogler, 2006; Mutailipu et al., 2024; Wang et al., 2024).

Table 1. *Studies related to Na_2CO_3 synthesis using CO_2 gas as the main raw material*

Material used	Operational Conditions	Optimum condition, products or conversions achieved	References
CO_2 from coconut shell combustion and NaOH solution.	Direct contact with NaOH at a concentration of 5–8 M, atmospheric pressure, and room temperature.	Optimal conditions were achieved at 7 M NaOH solution with Na_2CO_3 product amount of 190.6 grams/20 liters of solution or equivalent to 9.53 grams liter of NaOH solution.	Simanjuntak et al. (2014)
NaOH solution, Na_2CO_3 and NaCl solution.	Attempting to separate a mixture of NaCl, NaOH, Na_2CO_3 product, which is carried out at an operating temperature of 20–40°C (illustration of the separation process of the reaction products between CO_2 and NaOH).	The membrane separation of Na_2CO_3 product proceeded well and effectively.	Salmón et al. (2017)
Flue gas from power plant chimney.	NaOH concentration of 0.1–1 M and atmospheric pressure.	There is no information on the quantity of Na_2CO_3 product, but the characteristic results using Scanning Electron Microscopy – Energy Dispersive X-ray Spectroscopy (SEM-EDX) and X-ray Diffraction (XRD) show that Na_2CO_3 product was formed.	Guchhait et al. (2022)
CO_2 and NaOH solution.	CO_2 flow rate 20–500 ml/min., NaOH solution pH 12.7–13.7, reaction temperature 25°C, and atmospheric reaction pressure.	The conductivity test results of the reaction solution compared to standard Na_2CO_3 and $NaHCO_3$ solutions indicate that Na_2CO_3 product was formed, but an intermediate product in the form of $NaHCO_3$ was still present. However, there is no information about the quantity of either Na_2CO_3 or $NaHCO_3$ products.	Kuliyev et al. (2023)
CO_2 from air and NaOH solution.	NaOH concentration 3–30wt%, CO_2 concentration 0.0153–1.2 vol%, reaction temperature 5–20°C, CO_2 gas circulation flow: 0.4–1.6 L/min.	Optimal conditions were obtained at 6wt% NaOH concentration, reaction temperature of 20°C with the highest mass transfer coefficient, and Na_2CO_3 product was formed (no information on the quantity of product produced).	Ghaffari et al. (2023)
CO_2 and Na_2SiO_3 solution.	CO_2 gas flow rate 1.037–2.26 L/min., and sodium silicate (Na_2SiO_3) concentration 5–10wt%.	The optimum condition was achieved at a CO_2 gas flow rate of 1.648 L/minute and sodium silicate solution concentration of 10wt%, with the resulting Na_2CO_3 product yield of only 25.63%.	Ali and Ibrahim (2024)

$$y_{CO_2}P = H_{CO_2-H_2O}\, x_{CO_2} \tag{7}$$

$$k_1 \; or \; k_2 = A\, e^{\frac{-Ea}{RT}} \tag{8}$$

$$S_h = 2 + 0.6\, Re^{1/2}\, Sc^{1/3} \tag{9 a}$$

$$S_h = \frac{k_d\, L}{D} \tag{9 b}$$

$$Re = \frac{\rho\, N d_{imp}^2}{\mu} \tag{9 c}$$

$$Sc = \frac{\mu}{\rho\, D} \tag{9 d}$$

$$\frac{D}{\delta} \approx k_d \tag{10}$$

where y_{Co2} – molar fraction of CO_2 in gas phase (unitless); x_{Co2} – molar fraction of CO_2 in liquid phase (unitless); $H_{CO2\text{-}H2O}$ – Henry constant CO_2 – H_2O (Pa); P – system pressure (Pa); Sh – Sherwood number (unitless); Re – Reynolds (unitless); ρ (g/dm^3) – density, μ – viscosity (Pa.s); d_{imp} – impeller diameter (dm); Sc – Schmidt number (unitless); kd – mass transfer rate constant (m/s); N – stirring speed (rpm). A – collision frequency (order 1 (1/s) and order 2 (L/mol·s)); Ea – Activation energy (J/mol); R – Universal gas constant (8.314 J/mol·K); T – Absolute temperature (K).

When the reaction system is pressurized and conducted above atmospheric pressure, there is a more significant potential for more CO_2 gas to dissolve (see *Equation (6)*) into the NaOH solution. Similarly, raising the temperature of the reaction system increases the values of either k_1 or k_2. Meanwhile, increasing the NaOH concentration (C_{NaOH}) directly affects the diffusion-reaction rate (see *Equation (6)*).

Integrating these factors can potentially increase the diffusion-reaction rate and increase the amount of Na_2CO_3 produced later. However, everything has a maximum point. Therefore, observation of the reaction condition integration needs to be carried out. When it has exceeded its optimum conditions, increasing reaction variables will no longer have an effect, and the process becomes no longer effective and efficient. Therefore, the purpose of this research is to analyze and investigate the extent of the influence of NaOH concentration, reaction temperature and stirring speed in a pressurized system on the Na_2CO_3 produced. The hope of this research is to complement information related to operating conditions from previous research so that effective, efficient, and economical operating conditions will be obtained for the synthesis of CO_2 and NaOH-based to Na_2CO_3 in the future.

Material and Methods

Raw materials and equipment

The raw material used is purified CO_2 gas – purchased from Gasindo Andalan Sukses Co., Ltd., Cilegon, Banten, Indonesia – with 99% purity. NaOH solution was made by dissolving MERCK-brand NaOH pellets, adjusted to a specific mass corresponding to a concentration range of 10–30%. The research equipment consists of a CO_2 gas cylinder, a regulator, a flow meter, an overhead magnetic stirrer, a heating mantle, a gas distributor, and a water tank to maintain system pressure. The research equipment can be seen in detail in *Fig. (2)*.

Fig. 2. *Schematic of research equipment for Na_2CO_3 synthesis from CO_2 gas and NaOH*

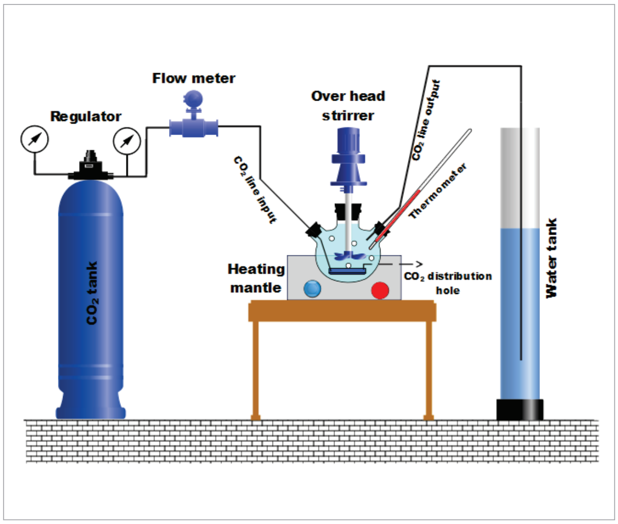

Experimental procedure

Add the NaOH solution at the predetermined concentration of 20–30wt% in 300 ml to the 3-neck flask. Fill the water tank with water to a height of 100 cm, equivalent to a hydrostatic pressure of 9.8 kPa. Turn on the heating mantle and regulate the solution's temperature until it reaches the target reaction range of 30–50°C. Activate the overhead magnetic stirrer and adjust it to the designated stirring speed (200 and 300 rpm). The next step is to open the regulator valve and adjust the CO_2 gas flow meter at 2 liters/minute. After 60 minutes, stop reaction process. Separate the reaction product from the liquid through a filtration process using filter paper. The solid retained on the filter paper is the reaction product, which is dried in an oven at 110°C for 2 hours to evaporate any remaining water in the product. The quantity of product obtained is calculated using *Equation (11)*.

$$M_{product} = m_0 - m_1 \tag{11}$$

where $M_{product}$ – mass of reaction product produced (gram); m_0 – mass of product + filter paper after oven drying (gram); m_1 – mass of empty filter papers (gram).

This research also attempted to model the reaction process using a mathematical model. This was done to predict and understand the phenomena occurring during the reaction process. Modelling was only performed under the best operating conditions, and the required data was the NaOH reduction data at reaction times of 0, 20, 40 and 60 minutes. The determination of NaOH content at specific reaction times using an acid-base titration method, using 0.1 N H_2SO_4 as the titrant. The NaOH content from the titration was calculated using *Equation (12)*.

$$C_{NaOH} = \frac{V_t.N.M_W}{V_s} \tag{12}$$

where C_{NaOH} – NaOH concentration at a specific time (mg/L); V_t – titrant volume (L); N – H_2SO_4 titrant normality (N); M_w – molecular weight (gram/mol); V_s – sample volume (L).

Characterization techniques

To determine whether the reaction product is Na_2CO_3, $NaHCO_3$, or a mixture of both, the dried sample was examined with Fourier Transform Infrared Spectroscopy (FTIR) using an Alpha II Bruker ATR instrument to monitor changes in functional group peaks. Spectra were collected over the 4000–500 cm^{-1} range at a resolution of 4 cm^{-1} with 32 scans. To confirm and reinforce the FTIR findings, Scanning Electron Microscopy (SEM) was performed on a Zeiss microscope under an accelerating voltage of 10.00 kV, a working distance (WD) of 8.58 mm, and 2.50 KX magnification. Before imaging, samples were sputter-coated with a thin gold layer to enhance surface conductivity and obtain clear morphological images. These combined analyses enabled precise observation of the surface morphology and microstructure, providing a definitive and reproducible identification of the products formed during the reaction.

Mathematical model testing

Further development of research to the pilot plant stage and even to the commercial stage requires a reaction rate constant (k). The reaction rate constant value is needed for reactor design and operation purposes. This study uses a simple mathematical model to predict the occurring phenomena, namely the Pseudo homogeneous model that refers to *Equation (5)*. However, several assumptions are applied. This is done to simplify the calculation process in the future applications. The assumptions are: 1. CO_2 is continuously introduced and stopped when the reaction time ends, so it can be assumed that stoichiometrically, CO_2 is in excess. Therefore, the reverse reaction is neglected assumption 2. The calculation approach is based on changes in NaOH concentration during the reaction process. Based on these two assumptions, *Equation (5)* can be simplified into *Equation (13)*.

$$-\frac{dC_{NaOH}}{dt} = k_1' \, C_{NaOH} \tag{13}$$

$$k_1' = 2 \, k_1 \, C_{CO_2} \tag{14}$$

Boundary conditions for the mathematical model are as follows:

- The initial concentration of NaOH at $t = 0$ is C_{NaOH_o}
- The reaction takes place in the liquid phase, and CO_2 gas is assumed to be evenly distributed at the interface under steady-state conditions.
- The stirring effect is assumed to be uniform at all positions, creating a homogeneous gas-liquid film.

Referring to *Equation (13)*, the model will be extended into first order and second order forms, which are commonly applied in predicting absorption behavior and general chemical reaction kinetics (Yasar and Kadhem, 2024).

Model of first order

The first-order model can be taken directly from *Equation (13)*, which is integrated to become *Equation (15)*.

$$\ln(C_{NaOH}) = \ln(C_{NaOH_o}) - k_1' \, t \tag{15}$$

Model of second order

In the second-order approach, *Equation (13)* is modified into *Equation (16)*.

$$-\frac{dC_{NaOH}}{dt} = k_1' \, {C_{NaOH}}^2 \tag{16}$$

When integrated, *Equation (16)* will be obtained.

$$\frac{1}{C_{NaOH}} = \frac{1}{C_{NaOH_0}} + k_1' t \qquad (17)$$

The validation of the mathematical model against the experimental data can be carried out in Microsoft Excel by analyzing the R^2 value (coefficient of determination) from the generated trendline. According to Tziotzios et al., (2024), a model is considered valid for representing the reaction process if the R^2 value is close to 1.

Results and Discussion

Effect of stirring speed

Fig. (3) shows that increasing the stirring speed positively impacts the product yield. When the stirring speed was increased from 200 rpm to 300 rpm, the amount of product obtained increased by 311.58% from the initial condition, from 3.28 grams at 200 rpm to 10.22 grams at 300 rpm. These results indicate that the increase in stirring has a significant effect on the diffusion rate (see *Equations (9a) – (10)* and *Equation (4)*). The increased stirring speed can reduce the diffusion resistance caused by the film layer (δ), resulting in a very high increase in diffusion rate. When related to *Equation (6)*, this phenomenon becomes very logical: when the diffusivity rate increases, it is followed by an increase in reaction rate and product yield.

The trend in this research shows similarities with the study conducted by Atmani et al., (2024), specifically in the color removal process performed at stirring speeds of 100 and 700 rpm. The results of Atmani et al., (2024) showed that the percentage of color removal increased from 71% to 83.4%. This means that the effect produced by increasing the stirring speed significantly influences the diffusion process and chemical reactions that occur.

Effect of NaOH concentration

The increase in NaOH concentration in the solution within the reaction system leads to an increase in the product yield (see *Fig. (4)*). In sequence, for NaOH concentrations of 10, 20, and 30wt%, the product masses obtained were 10.22, 13.18, and 13.78 grams. Increasing the NaOH concentration variable in the solution will increase diffusion and reaction rates (*Equation (6)*) due to its direct proportion to the change in reactant concentration. From a molecular perspective, increasing the NaOH concentration at constant temperature and stirring speed enhances the Brownian motion of NaOH molecules (Oreyeni et al., 2024), which in turn increases the collision frequency (A). This directly affects the reaction rate constant as shown in *Equation (8)*.

The results of this study are reinforced by research conducted by Michelson et al., (2024) on CO_2 capture observations. NaOH concentration variation was performed by adding NaOH to the solution to maintain pH in the range of 8–14, which showed that increasing solution pH (increasing NaOH concentration) had a positive impact on increasing CO_2 absorption efficiency.

Fig. 3. *Effect of stirring speed at system temperature of 30°C and NaOH concentration 10wt%*

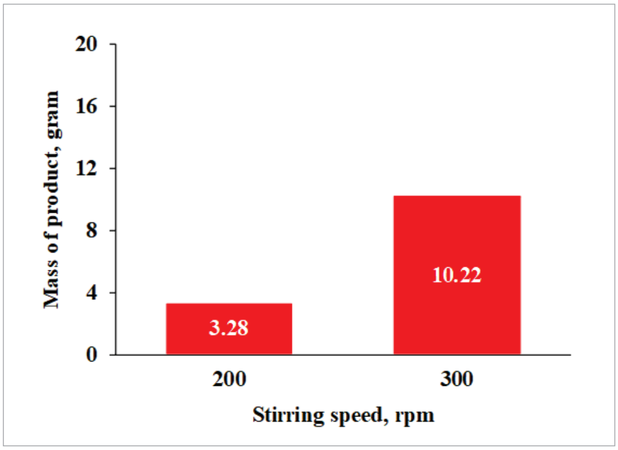

Fig. 4. *Effect of NaOH concentration at reaction temperature of 30°C and stirring speed of 300 rpm*

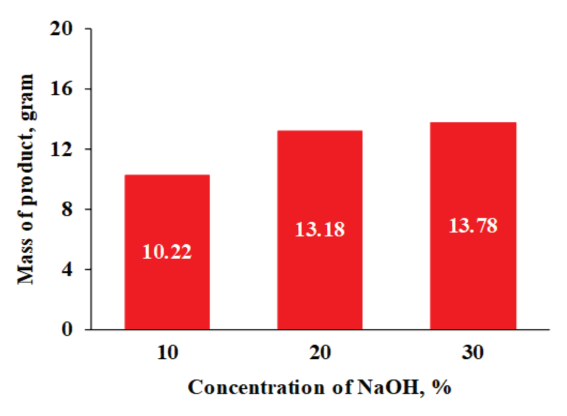

These results prove that increasing NaOH concentration in CO_2 and NaOH contact positively impacts the absorption process. However, when observing *Fig. (4)*, the increase in product yield was not as significant as with the stirring speed variable (see *Fig. (3)*). At NaOH concentrations from 10wt% to 20wt%, the product yield only increased by 2.96 grams, and subsequently, from NaOH concentration 20wt% to 30wt% only increased by 0.6 grams. This phenomenon is likely because NaOH in the reaction system has reached maximum interaction with CO_2 to form products (referring to *Equations 2–3*). To increase the reaction product yield (sodium carbonate), it may be possible to increase NaOH concentration above 30wt% and vary the CO_2 flow rate to determine the dominance level of impact (whether NaOH concentration or CO_2 flow rate) on the reaction results obtained; however, while ensuring that the product formed is Na_2CO_3 rather than $NaHCO_3$.

Effect of reaction temperature

As shown in *Fig. (5)*, increasing the reaction temperature in the reaction system leads to an increase in reaction rate, as evidenced by the mass of the product obtained. These results align with the concepts in *Equation (8)* and *Equation (5)*. When the reaction temperature is raised, the reaction rate constant increases, leading to an increase in the reaction rate between CO_2 and NaOH. The sequential increase in product mass obtained was 13.78, 15.14, and 16.43 grams for reaction temperatures of 30, 40, and 50°C. Based on another concept referring to the Wilke-Chang equation (Bird et al., 2007), increasing reaction temperature reduces the viscosity of the NaOH solution. This condition causes the diffusion rate of CO_2 into the NaOH solution to increase as the external resistance in the form of a film layer decreases due to the increase in system temperature (see *Equations (9a) – (10)*). This condition leads to enhanced interaction between CO_2 and NaOH, followed by an increased reaction rate.

This study produced significantly higher yields than the results of research conducted by Simanjuntak et al., 2014. The research by Simanjuntak et al., 2014 only achieved 9.53 grams/liter of NaOH solution (see Table 1), while this study achieved 16.43 grams/300 ml of NaOH solution, equivalent to 54.77 grams/liter of NaOH solution (a difference of 5.75 times or 575%). Thus, implementing a pressurized system integrating influential factors has proven successful, effective, and efficient. To verify this success, a detailed analysis was conducted regarding NaOH concentration changes over time, measured at reaction times of 0, 20, 40 and 60 minutes. As shown in *Fig. (6a)* and *Fig. (6b)*, the NaOH concentration decreased significantly from 1.28 mg/L to 0.09 mg/L (from reaction time 0 to 60 minutes). When converted, the NaOH converted product amounts to 93.36%. Therefore, the integration of NaOH concentration, reaction temperature, and stirring speed in the pressurized reaction system for Na_2CO_3 production in this study has been successful. Based on the trends shown in *Fig. (6)*, if the reaction time were extended beyond 60 minutes, NaOH conversion could reach 100%.

Fig. 5. *Effect of reaction temperature at stirring speed of 300 rpm and NaOH concentration of 30wt%*

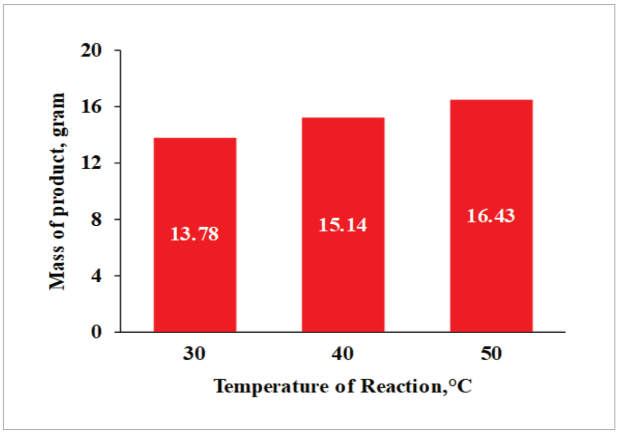

Based on observations at a reaction temperature of 50°C (see *Fig. (5)*), where a high product yield of 16.43%/300 ml of NaOH solution was achieved, CO_2 capture using NaOH shows strong potential as a sustainable carbon emission management strategy. The process can be integrated into industries that emit CO_2, such as power plants, cement production, petrochemical industries and metal processing. In addition to reducing emissions, this integration also produces commercially valuable Na_2CO_3, which can be reused in chemical manufacturing, water treatment, and other industrial applications. This approach supports both carbon capture and utilization (CCU) and the circular economy.

Testing of reaction kinetics model

The reaction-kinetics calculations in this study were carried out under the optimum conditions: a stirring speed of 300 rpm, an NaOH concentration of 30%, and a reaction temperature of 50°C. *Fig. (4)* shows that when the NaOH concentration was raised from 20% to 30%, the product yield increased only from 13.18% to 13.78%. This suggests that stirring no longer meaningfully affects diffusion and that external mass transfer resistance is negligible. In *Fig. (5)*, raising the reaction temperature from 30°C to 50°C increased the product mass from 13.78 grams to 16.43 grams, indicating that temperature strongly influences the reaction rate in accord with the Arrhenius principle. Given the data in *Fig. (4)* and *Fig. (5)*, it is reasonable to model the system by neglecting diffusion effects and assuming kinetic control. Nonetheless, further work should explore the influence of stirring speed over a wider range (above 300 rpm) while keeping the NaOH concentration constant, so that future trends can be established with greater certainty.

Based on *Fig. 7(a)* and *Fig. 7(b)* (derived from the data processing in *Fig. 6(a)* and *Fig. 6(b)*, particularly *Fig. 6(a))* the trendline results using Microsoft Excel for first order and second order kinetic models show that the R^2 value for first order is closer to 1 than for second order, with values of 0.9901 and 0.8291, respectively. This data indicates that the reaction between CO_2 and NaOH follows first-order kinetics, and the approach taken with several assumptions is sufficiently valid. Thus, the increase in reaction rate in this study is proportional to the increase in NaOH concentration.

Based on the trendline and the equation shown in *Fig. (7a)*, corresponding to *Equation (15)*, the calculated value is 0.0455 per minute. This indicates that 4.55% of NaOH reacts with CO_2 gas every minute.

Fig. 6. *Effect of reaction temperature on: (a) NaOH decrease in the reaction system, (b) on the resulting reaction conversion*

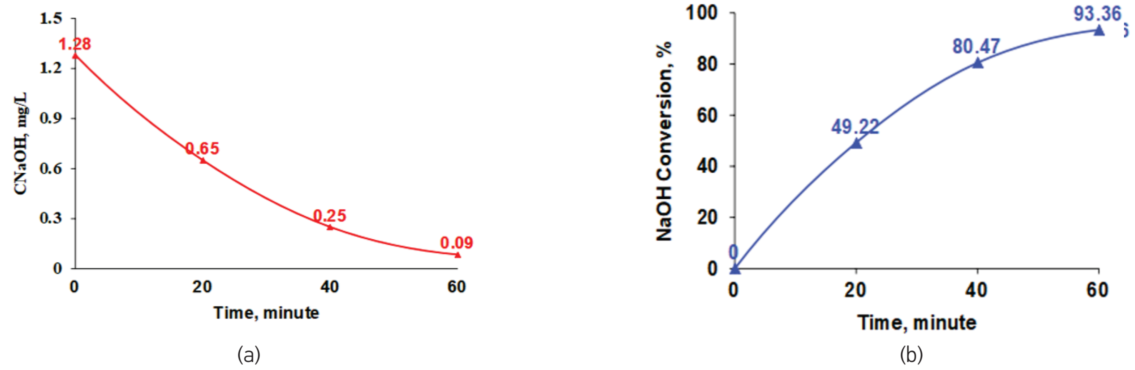

(a) (b)

Fig. 7. *Effect of reaction temperature on: (a) first order, (b) second order*

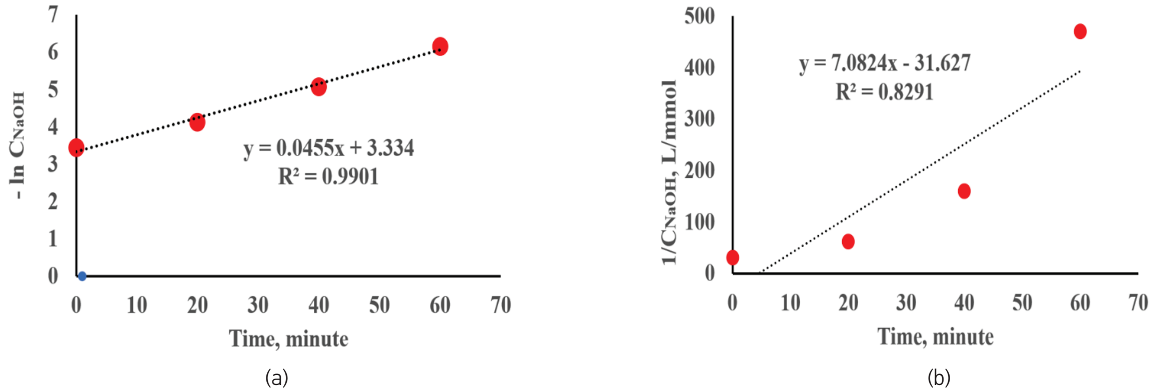

(a) (b)

Testing of reaction product characteristics

Fig. (8a) and *Fig. (8b)* shows that the peaks appearing in the FTIR analysis of the reaction products at 10wt% NaOH concentration versus 30% NaOH concentration produced different peaks. When compared to standard FTIR spectra from established references, specifically for $NaHCO_3$ and Na_2CO_3 (as reported by the NIST (2023), the product formed at a 10% NaOH concentration shows FTIR peaks that more closely match those of standard $NaHCO_3$ than those of standard Na_2CO_3. Meanwhile, at 30wt% concentration (*Fig. (8b)*), the emerging peaks are almost 100% similar to Na_2CO_3. Referring to the concept in *Equation (1)*, these FTIR test results are logical because the availability of NaOH in the reaction system is higher at 30wt% NaOH concentration compared to 10wt% NaOH concentration. This condition allows $NaHCO_3$, which is an intermediate product, to react again with the NaOH present in the reaction system to continue the reaction, forming Na_2CO_3 (see *Equations (2)* and *(3)*). However, when the availability of NaOH in the system is very low, the reaction stops, and the final product has a composition containing more $NaHCO_3$ compared to the main product, Na_2CO_3.

The SEM testing results reinforce the findings from the FTIR test (see *Fig. (9a)* and *Fig. (9b)*). The SEM results revealed clear differences, with *Fig. (9a)* showing a large number of small rod-shaped crystals that are morphologically consistent with $NaHCO_3$ (Crampon et al., 2023). In contrast, *Fig. (9b)* morphologically contains very few tiny rod-shaped crystals and is dominated by crystals with flat and smooth morphology, and this is identical to Na_2CO_3 (Wang et al., 2019; Simanjuntak et al., 2014). *Fig. (9a)* and *Fig. (9b)* indicate that if the desired main product is Na_2CO_3, it should be carried out at approximately 50°C and a NaOH concentration ≥ 30*wt*%.

Fig. 8. *Scanning electron microscopy (FTIR) test results: (a) NaOH concentration 10wt%, (b) concentration 30wt% at reaction temperature of 50°C*

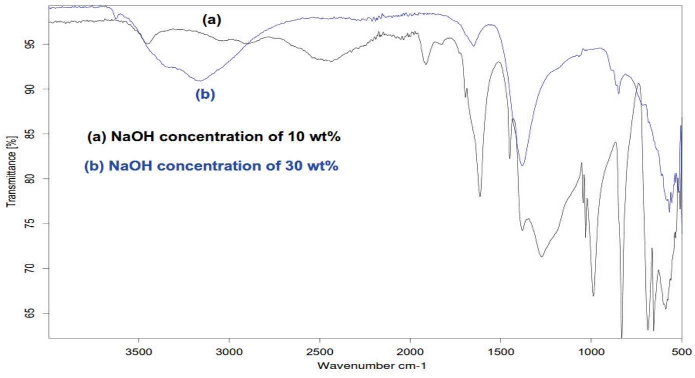

Fig. 9. *Scanning Electron Microscopy (SEM): (a) NaOH concentration 10wt%, (b) concentration 30wt% at reaction temperature of 50°C*

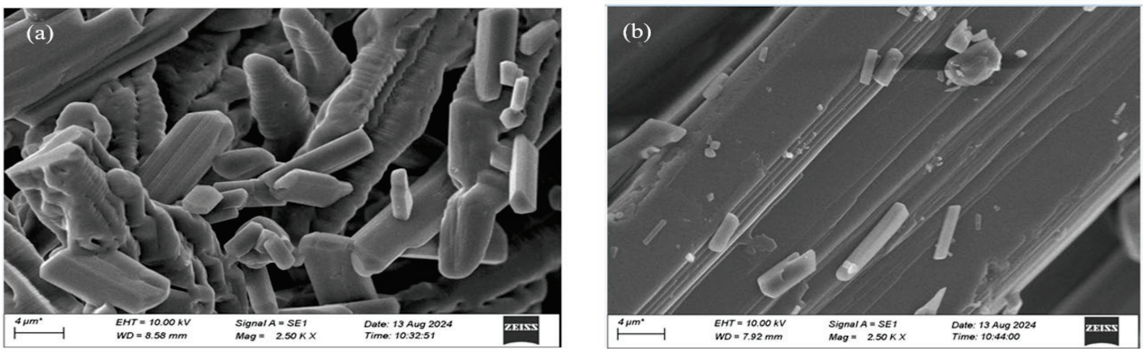

Conclusions

The combination of pressurized system (9.8 kPa) and a stirred process used in this study, integrated with other influential absorption factors such as NaOH absorbent concentration and system temperature, had a positive impact on CO_2 capture performance. Increases in NaOH concentration, stirring speed, and system temperature enhanced the diffusion-reaction rate, as evidenced by the increase in product yield and conversion. Notably, at a temperature of 50°C, NaOH concentration of 30wt%, and stirring speed of 300 rpm, the process was able to convert up to 93.36% of NaOH within 60 minutes, producing a product identical to Na_2CO_3.

The pressurized reaction system in this research compared to without pressure in references significantly affects the sodium carbonate product produced, increasing it by 5.75 times or 575%. In terms of chemical reaction rate, this research follows a first-order mathematical model with an R^2 value approaching 0.9901 with a value of 0.0455 minutes^{-1}. The best conditions in this research were achieved at a stirring speed of 300 rpm, NaOH concentration of 30wt%, and reaction temperature of 50°C with a product amount of 16.43 grams.

Given the success of this research, the pressurized reaction method has the potential for further development to pilot plant scale in the future and requires further observation. In general, the integration of factors shows success, but further observations are still needed, particularly the collaboration of NaOH concentration-CO_2 gas flow rate variables to obtain a more economical reaction process and produce Na_2CO_3 with 100% purity.

Acknowledgements

The authors would like to express their sincere gratitude to the Department of Chemical Engineering, Faculty of Engineering, Universitas Sultan Ageng Tirtayasa, for supporting research facilities and infrastructure. We hope this research will benefit the general public and advance science.

References

Ali D. A. and Ibrahim M. E. (2024) Optimization Using Central Composite Design for Continuous Absorption of CO_2 gas with Green Sodium Silicate in a Packed Bed Column. Heliyon 10(12): e32953. Available at: https://doi.org/10.1016/j.heliyon.2024.e32953

Al-Mamoori A., Hameed M., Saoud A., Al-ghamdi T., Al-Naddaf Q., ALwakwak A. A., and Baamran K. (2023) Development of Sodium-Based Borate Adsorbents for CO_2 Capture at High Temperatures. Industrial and Engineering Chemistry Research 62(8): 3695-3704. Available at: https://doi.org/10.1021/acs.iecr.2c04129

Atmani F., Kaci M. M., Yeddou-Mezenner N., Soukeur A., Akkari I., and Navio J. A. (2024) Insights into the physicochemical properties of Sugar Scum as a sustainable biosorbent derived from sugar refinery waste for efficient cationic dye removal. Biomass Conversion and Biorefinery 14(4): 4843-4857. Available at: https://doi.org/10.1007/s13399-022-02646-3

Bird R. B., Stewart W. E., and Lightfoot E. N. (2002) Transport phenomena (2nd ed.). John Wiley and Sons.

Chan R. Y., Zeng Y. Z., Hou C. C., Kuo H. C., and Huang H. W. (2025) Experimental study of carbon dioxide capture and mineral carbonation using sodium hydroxide solution. Journal of Ecological Engineering 26(1): 30-45. Available at: https://doi.org/10.12911/22998993/195214

Couespel D., Lévy M., and Bopp L. (2024) Stronger Oceanic CO_2 Sink in Eddy-Resolving Simulations of Global Warming. Geophysical Research Letters 51(4): e2023GL106172. Available at: https://doi.org/10.1029/2023GL106172

Crampon C., Detoisien T., Itani L., Nicolas F., Myotte E., and Badens E. (2023) Novel crystal morphology for sodium bicarbonate obtained by using the supercritical anti-solvent process. Powder Technology 418: 118313. Available at: https://doi.org/10.1016/j.powtec.2023.118313

Evans H. A., Carter M., Zhou W., Yildirim T., Brown C. M., and Wu H. (2024) Water-enhanced CO 2 capture with molecular salt sodium guanidinate. Journal of Materials Chemistry A 12(27): 16748-16759. Available at: https://doi.org/10.1039/D4TA03037K

Fogler H. S. (2006) Elements of chemical reaction engineering (4th ed.). Pearson Education.

Ghaffari S., Gutierrez M. F., Seidel-Morgenstern A., Lorenz H., and Schulze P. (2023) Sodium hydroxide-based CO_2 direct air capture for soda ash production – fundamentals for process engineering. Industrial and Engineering Chemistry Research 62(19): 7566-7579. Available at: https://doi.org/10.1021/acs.iecr.3c00357

Guchhait S. K., Yadav K. K., Khatana S., Saini R. K., Arora U. K., Satyakam R., and Jha M. (2022) Conversion of gaseous effluents of power plant to sodium carbonate: A value-added material for powder detergent. Cleaner Waste Systems 3: 100042. Available at: https://doi.org/10.1016/j.clwas.2022.100042

Kuliyev S., Tas Y. E., and Selim Cogenli M. (2023) Control of CO_2 Absorption by NaOH Solution Using pH, Conductivity, and Titration Measurement. Kimya Problemleri 21(2): 123-131. Available at: https://doi.org/10.32737/2221-8688-2023-2-123-131

Michelson J., Mäki-Arvela P., Rajala P., Hallapuro M., Schmid D., Karlström O. and Murzin D. Y. (2024) Modeling of a bubble column for CO_2 removal by absorption with NaOH. Chemical Engineering Communications 211(4): 571-581. Available at: https://doi.org/10.1080/00986445.2023.2261105

Mutailipu M., Song Y., Yao Q., Liu Y., and Trusler J. M. (2024) Solubility and interfacial tension models for CO_2-brine systems under CO2 geological storage conditions. Fuel 357: 129712. Available at: https://doi.org/10.1016/j.fuel.2023.129712

NIST (National Institute of Standards and Technology) (2023) Sodium carbonate. NIST Chemistry WebBook, SRD 69. Available at: https://webbook.nist.gov/cgi/cbook.cgi?ID=C497198&-Type=IR-SPEC&Index=1 (accessed 01 December 2024).

NIST (National Institute of Standards and Technology) (2023) Sodium bicarbonate. NIST Chemistry WebBook, SRD 69. Available at: https://webbook.nist.gov/cgi/cbook.cgi?ID=B6000512&Mask=80 (accessed 01 December 2024).

Ozerdem S. and Ozerdem M. S. (2024) Calculating the Carbon Footprint for Environmental Sustainability: The Case of Ted Diyaabakir College (Turkiye). Profresional Studies: Theory And Practice 28(1): 80-89. Available at: https://doi.org/10.56131/pstp.2024.28.1.257

Oreyeni T., Shamshuddin M. D., Obalalu A. M., Saeed A., and Shah N. A. (2024) Exploring the impact of stratification on the dynamics of bioconvective thixotropic fluid conveying tiny particles and Cattaneo-Christov model: Thermal storage system application. Propulsion and Power Research 13(3): 416-432. Available at: https://doi.org/10.1016/j.jppr.2024.08.002

Plaza P., Usall J., Torres R., Abadias M., Smilanick J. L., and Vinas I. (2004) The use of sodium carbonate to improve curing treatments against green and blue moulds on citrus fruits. Pest Management Science: formerly Pesticide Science 60(8): 815-821. Available at: https://doi.org/10.1002/ps.880

Prajapati M., Thesia D., Thesia V., Rakholia R., Tailor J., Patel A. and Shah M. (2024) Carbon capture, utilization, and storage (CCUS): a critical review towards carbon neutrality in India. Case Studies in Chemical and Environmental Engineering 10: 100770. Available at: https://doi.org/10.1016/j.cscee.2024.100770

Rogelj J. and Lamboll R. D. (2024) Substantial reductions in non-CO_2 greenhouse gas emissions reductions implied by IPCC estimates of the remaining carbon budget. Communications Earth and Environment 5(1): 35. Available at: https://doi.org/10.1038/s43247-023-01168-8

Rubangakene N. O., Elwardany A., Fujii M., Sekiguchi H., and Shokry H. (2023) Influence of Impregnation of Sodium Carbonate Catalyst on Physicochemical Properties of Biochar. Engineering Proceedings 37(1): 77. Available at: https://doi.org/10.3390/ECP2023-14688

Salmón I. R., Janssens R., and Luis P. (2017) Mass and heat transfer study in osmotic membrane distillation-crystallization for CO_2 valorization as sodium carbonate. Separation and Purification Technology 176: 173-183. Available at: https://doi.org/10.1016/j.seppur.2016.12.010

Simanjuntak W., Sembiring S., Zakaria W. A., and Pandiangan K. D. (2014) The use of carbon dioxide released from coconut shell combustion to produce Na_2CO_3. Makara J. Sci 18(3): 65-70. Available at: https://doi.org/10.7454/mss.v18i3.3717

Tziotzios G., Pantazi X. E., Paraskevas C., Tsitsopoulos C., Valasiadis D., Nasiopoulou E. and Molassiotis A. (2024). Non-Destructive Quality Estimation Using a Machine Learning-Based Spectroscopic Approach in Kiwifruits. Horticulturae 10(3): 251. Available at: https://doi.org/10.3390/horticulturae10030251

Wang Y., He F., Wang J., and Hu Q. (2019) Comparison of effects of sodium bicarbonate and sodium carbonate on the hydration and properties of Portland cement paste. Materials 12(7): 1033. Available at: https://doi.org/10.3390/ma12071033

Wang Z., Christodoulou C., and Mazzei L. (2024) Analytical study on the liquid-particle mass transfer coefficient for multiparticle systems. Chemical Engineering Journal 494: 152733. Available at: https://doi.org/10.1016/j.cej.2024.152733

Yasar M. and Kadhem A. A. (2024) Investigating the Role of Aluminum Doping on the Bandgap Modulation and Photocatalytic Efficiency of Strontium Nickel Ferrites for Ciprofloxacin Degradation. Arabian Journal for Science and Engineering: 1-15. Available at: https://doi.org/10.1007/s13369-024-09604-3
